The Journal of Physiology

Contractile properties of developing human fetal cardiac muscle

Alice W. Racca[1], Jordan M. Klaiman[1], J. Manuel Pioner[2], Yuanhua Cheng[1], Anita E. Beck[3,4], Farid Moussavi-Harami[5], Michael J. Bamshad[3,4] and Michael Regnier[1,6,7]

[1] *Department of Bioengineering, University of Washington, Seattle, WA, USA*
[2] *Department of Experimental and Clinical Medicine, Division of Physiology, University of Florence, Italy*
[3] *Department of Pediatrics, University of Washington, Seattle, WA, USA*
[4] *Seattle Children's Hospital, Seattle, WA, USA*
[5] *Division of Cardiology, Department of Internal Medicine, University of Washington, Seattle, WA, USA*
[6] *Institute for Stem Cell and Regenerative Medicine, University of Washington, Seattle, WA, USA*
[7] *Center for Cardiovascular Biology, University of Washington, Seattle, WA, USA*

Key points

- The contractile properties of human fetal cardiac muscle have not been previously studied.
- Small-scale approaches such as isolated myofibril and isolated contractile protein biomechanical assays allow study of activation and relaxation kinetics of human fetal cardiac muscle under well-controlled conditions.
- We have examined the contractile properties of human fetal cardiac myofibrils and myosin across gestational age 59–134 days.
- Human fetal cardiac myofibrils have low force and slow kinetics of activation and relaxation that increase during the time period studied, and kinetic changes may result from structural maturation and changes in protein isoform expression.
- Understanding the time course of human fetal cardiac muscle structure and contractile maturation can provide a framework to study development of contractile dysfunction with disease and evaluate the maturation state of cultured stem cell-derived cardiomyocytes.

Abstract Little is known about the contractile properties of human fetal cardiac muscle during development. Understanding these contractile properties, and how they change throughout development, can provide valuable insight into human heart development, and provide a framework to study the early stages of cardiac diseases that develop *in utero*. We characterized the contractile properties of isolated human fetal cardiac myofibrils across 8–19 weeks of gestation. Mechanical measurements revealed that in early stages of gestation there is low specific force and slow rates of force development and relaxation, with increases in force and the rates of activation and relaxation as gestation progresses. The duration and slope of the initial, slow phase of relaxation, related to myosin detachment and thin filament deactivation rates, decreased with gestation age. F-actin sliding on human fetal cardiac myosin-coated surfaces slowed significantly from 108 to 130 days of gestation. Electron micrographs showed human fetal muscle myofibrils elongate and widen with age, but features such as the M-line and Z-band are apparent even as early as day 52. Protein isoform analysis revealed that β-myosin is predominantly expressed even at the earliest time point studied, but there is a progressive increase in expression of cardiac troponin I (TnI), with a concurrent decrease in slow skeletal TnI. Together, our results suggest that cardiac myofibril force production and kinetics of activation and relaxation change significantly with gestation age and are influenced by the structural maturation of the sarcomere and changes in contractile filament protein isoforms.

DOI: 10.1113/JP271290

(Received 16 July 2015; accepted after revision 6 October 2015; first published online 13 October 2015)
Corresponding author M. Regnier: UW Medicine Research, 850 Republican Street, Box 358056, Seattle, WA 98109, USA. Email: mregnier@uw.edu

Abbreviations cTnI, cardiac troponin I; F_{MAX}, the specific active force produced at maximal calcium concentration; F_{PASS}, the specific passive force measured in relaxing solution; $F_{pCa5.8}$, the specific active force produced in pCa 5.8 solution; HMM, heavy meromyosin; k_{ACT}, the rate of force development; $k_{REL,fast}$, the rate of the fast phase of relaxation; $k_{REL,slow}$, the normalized slope of the slow phase of relaxation; MHC, myosin heavy chain; ssTnI, slow skeletal troponin I; $t_{REL,slow}$, the duration of the slow phase of relaxation; $t_{REL,50}$, the time at which 50% of total relaxation is reached; $t_{REL,90}$, the time at which 90% of total relaxation is reached; V_f, speed of F-actin filaments in the *in vitro* motility assay; V_{MAX}, maximum velocity of F-actin filaments in the *in vitro* motility assay.

Introduction

The contractile properties of human fetal cardiac muscle have not yet been described and functional information has been primarily obtained via studies *in vivo* with echocardiography. Most of what is known about the contractile properties of developing mammalian cardiac muscle comes from experiments in animal models. However, these studies are limited in their applicability to human cardiac development because of differences in the temporal pattern and the composition of contractile protein isoform expression.

As the human fetal heart ages, the longitudinal shortening (ratio of atrioventricular plane displacement to left ventricular length) decreases (Elmstedt *et al.* 2012) and the left ventricle end diastolic volume increases (Luewan *et al.* 2014; Brooks *et al.* 2014). Heart rate decreases as the fetus grows, while diastolic filling and atrial contraction durations, and the peak velocities of the septum, atrial contraction and ventricle ejection all increase (Elmstedt *et al.* 2013). However, conclusions from these studies are limited by a lack of *ex vivo* quantitative muscle contractile studies, and thus cannot decouple the effects of Ca^{2+} handling and whole cell maturation from the function of the myofilament proteins. It is unknown if the changes in gross contraction of the heart are a result of protein isoform expression pattern changes, structural development or changes to the Ca^{2+} handling apparatus.

Ex vivo studies on human fetal heart tissue report significant changes in morphology, ultrastructure and protein composition as the fetus develops. The gross morphology of the heart undergoes considerable change through the first 112 days of development, including septation (separating the left and right halves between 35 and 53 days of gestation), formation of the valve components between 49 and 56 days, and delamination of the leaflets into the tricuspid valve between 56 and 112 days (Lamers *et al.* 1995). At 119 days, there are few myofibrils in the heart and they are scattered, very short, with thick z-bands and are loosely packed (Kim *et al.* 1992); however, there is no information on the ultrastructure of cardiomyocytes before this time point. Previous studies have shown that several key contractile protein isoforms change in expression levels between 49 days and full-term gestation. The human fetal heart ventricle shows a marked decrease in the small amount of α-myosin heavy chain (α-MHC) between 47 and 110 days of gestation (Reiser *et al.* 2001). Moreover, slow skeletal troponin I (ssTnI) is the predominant TnI isoform expressed in the heart from as early as 63 days of gestation to 12 weeks after birth (Sasse *et al.* 1993). The continued expression of ssTnI may lead to slower overall ATPase activity (Anderson *et al.* 1991; Purcell *et al.* 1999).

The contractile properties of the developing human fetal heart probably change over time due to this complex combination of protein isoform expression changes and the structural maturation of sarcomeres. An in-depth study of the function of the developing myocardium is needed to better understand the developmental process of the heart and create better informed hypotheses regarding the dysfunction that occurs in disease development from structural abnormalities or genetic mutations within the heart. Knowledge of the contractile properties of human fetal cardiac muscle could also help to identify potential avenues for early intervention into cardiac muscle diseases that develop *in utero*.

Here we provide an initial report of the mechanical and structural properties of human fetal left ventricle myofibrils (the contractile organelles of striated muscle cells) and isolated myosin, using isolated myofibril preparations and purified actin and myosin (heavy meromyosin; HMM) in an *in vitro* motility assay. In agreement with reports by others (Sasse *et al.* 1993; Reiser *et al.* 2001), throughout the age range studied (52 to 134 days of gestation), the fetal cardiac muscle predominantly expresses the β-myosin heavy chain (β-MHC), and there is a progressive increase in the relative proportion of cardiac TnI (cTnI) to the total amount of TnI present throughout gestation. We report that human fetal myofibrils produce more force and have faster activation and relaxation kinetics as they develop, and this is correlated with maturation of sarcomere structure and myofibril alignment. Unregulated F-actin filament sliding velocity (V_f) on human fetal cardiac myosin decreased with age, in agreement with a decrease in cross-bridge detachment rate estimated from the early, slow phase of relaxation in

Table 1. Fetal samples arranged by age, with experimental information

No.	Sample age (days)	Sample sex	Self-reported ethnicity	Myofibrils (no.)	*In vitro* motility	Electron microscopy imaging
1	52	n/a	n/a	0 successful		x
2	59	n/a	n/a	5		
3	74	female	Caucasian	5		
4	101	female	Hispanic	12	x	
5	105	female	Caucasian	9		
6	107	male	Alaskan Native/ Caucasian	4		
7	108	n/a	n/a			x
8	110	male	African American	3		
9	110	female	Caucasian	9		
10	114	male	Native American	7		
11	115	male	Caucasian		x	
12	115	female	African American	10		
13	116	female	n/a	23	x	
14	127	male	n/a			x
15	130	male	Asian	7		
16	130	female	Caucasian	1		
17	134	male	Asian (Korean)	4		

myofibrils. The V_f of fetal cardiac myosin at 134 days is close to the speed of human adult left ventricle myosin (Moussavi-Harami *et al.* 2015). Our study is an important step towards improved understanding of the development of the human fetal heart contractile properties and we conclude that the fetal left ventricle increases in force production magnitude and speed as it ages from 52 to 134 days of gestation. A preliminary report of this work were presented in abstract form (Racca *et al.* 2014).

Methods

Ethical approval and tissue preparation

Normal human fetal tissue was obtained by the Laboratory of Developmental Biology at the University of Washington with Internal Review Board approval from the University of Washington and Seattle Children's Research Institute, using standards set by the latest revision of the Declaration of Helsinki. Laboratory personnel from the Laboratory of Developmental Biology collected specimens at clinics, where a short time after passage in cold phosphate solution, the specimens were examined, sexed and aged (calculating the age in post-conception days). The age range of fetuses for this project was 52–134 days of gestation (see Table 1 for a list of samples). Samples were stored in PBS at 4°C until dissection, for a period of 2–6 h. The heart was identified and pieces of the outer wall of the left ventricle were removed and placed immediately into a skinning solution [relaxing solution with 50% glycerol (by volume) and 1% Triton X-100, as previously described (Brenner & Eisenberg, 1986; Regnier *et al.* 2000; Korte *et al.* 2012)]. For the samples which were 52, 59 and 74 days of gestation, both the ventricles and the septum may have been utilized. For a subset of samples, following identification of the heart, sections of the left ventricle were placed in 4% glutaraldehyde for electron microscopy imaging. Because of the limited size of the samples, samples used for electron microscopy were not able to be used for contractile assays. Overall, 17 samples were acquired and used in this project, collected over a period of 14 months.

Adult heart tissue was obtained following written informed consent from eight patients who were undergoing cardiac placement of a left ventricular-assist device (7/8) or cardiac transplantation (1/8) for end stage heart failure under a study protocol approved by the University of Washington Institutional Review Board. Samples were transported to the laboratory in cold PBS solution and immediately prepared for use as detailed in below. Full details of the patient study population were reported in a previous publication (Moussavi-Harami *et al.* 2015).

Solutions for myofibril mechanics

Solutions for myofibril mechanics experiments were made as previously described (Rao *et al.* 2014). Briefly, solution composition was computed by an iterative algorithm that calculates the equilibrium concentration of ligands and ions based on published affinity constants (Fabiato, 1988). Relaxing and activating solutions contained (in mM): 80 Mops, 15 EGTA, 1 Mg^{2+}, 5 MgATP, 83 K^+, 52 Na^+ and 15 creatine phosphate, pH 7.0 at 15°C; solution ionic strength was 170 mM. For adult myofibrils, the concentration of MgATP was 2 mM. The Ca^{2+} concentration (expressed as pCa = –log [Ca^{2+}]) was set by adjusting the amount of $CaCl_2$.

Myofibril mechanics

Muscle samples were demembranated for 24 h at 4°C in relaxing solution containing 50% glycerol (by volume) and 1% Triton X-100, as previously described (Brenner & Eisenberg, 1986; Regnier *et al.* 2000). The demembranated muscle tissue was then transferred to a 50% glycerol-relaxing solution and stored at –20°C for use up to 1 week.

To obtain isolated small bundles of myofibrils (average width of bundles 6.5 ± 0.2 μm), small pieces of muscle tissue were placed into rigor solution (in mM): 50 Tris, 100 KCl, 2 $MgCl_2$, 1 EGTA, 2 dithiothreitol (DTT), pH 7, containing a 1:200 dilution of protease inhibitor cocktail (Sigma-Aldritch, St. Louis, MO, USA). After two rinses in rigor solution, the tissue was shredded with a high speed homogenizer for one or two bursts of 15 s. Myofibrils were stored at 4°C and used within 3 days.

Myofibril experiments were performed as previously described (Colomo *et al.* 1997; Racca *et al.*, 2013, 2015; Moussavi-Harami *et al.* 2015).

Specific passive force was measured for a subset of preparations after stretching the myofibril bundle 10% above its resting length, which resulted in a sarcomere length of 2.3 μm. Activation and relaxation data were collected at 15°C and fit with linear regression as previously described (Kreutziger *et al.* 2008; Racca *et al.*, 2013, 2015). A $t_{1/2}$ estimation was used in place of a single-exponential fit because the rate of rise or fall in force was not well described by a single exponential, and this was converted to a rate using the equation: $1/t_{1/2}$ (Racca *et al.* 2013). Briefly, the activation rate (k_{ACT}; with rapid increase in Ca^{2+}) was estimated from the time to reach 50% maximal activation. Forces measured were standardized to cross-sectional area of the myofibril and reported as specific force (F_{MAX}, mN mm^{-2}). Relaxation rate for slow phase ($k_{REL,slow}$) was reported as the slope of a regression line fit to the tension trace and normalized to the tension amplitude, and the duration of the slow phase was measured from the onset of solution change at the myofibril to the shoulder marking the beginning of the fast phase. The transition from the slow to rapid phase was determined through multiple factors, including an apparent change in the slope of the data or a change in the signal-to-noise ratio which was often apparent at the transition (Fig. 1*B*). The relaxation rate for the fast phase ($k_{REL,fast}$) was estimated from the time to 50% reduction in force.

In vitro motility assay

Myosin and F-actin preparation. Cardiac myosin was prepared according to previously described methods and stored at 4°C in a storage solution (in mM: 600 KCl, 10 Tris, 2 $MgCl_2$, 5 DTT, pH 7.6) for up to 3 days (Margossian & Lowey, 1982). Aliquots of the myosin were digested to HMM by enzymatic digestion with tosyl lysine chloromethyl ketone (TLCK)–chymotrypsin (50 mg ml^{-1}; Sigma) (Kron *et al.* 1991*a*, *b*). HMM was prepared daily. The concentration of HMM and myosin was determined using spectrophotometry as previously described (Clemmens & Regnier, 2004). Rabbit skeletal F-actin was prepared from muscle ether powder, labelled with rhodamine–phalloidin (Molecular Probes, Eugene, OR, USA) as previously described (Pardee & Spudich, 1982; Spudich *et al.* 1982; Kron *et al.* 1991*a*, *b*), stored at 4°C and used within 6 weeks.

Flow cells were prepared as previously described (Gordon *et al.* 1997; Clemmens *et al.* 2005). Briefly, two glass coverslips, one 22 mm x 60 mm (VWR Scientific, West Chester, PA, USA) and one 18 mm^2 (Corning, Horseheads, NY, USA), were separated by 2 mm adhesive foam spacers. The larger coverslip surface was first cleaned and coated with 1% nitrocellulose in amyl acetate (Sigma) and allowed to dry.

F-actin filament velocity (V_f) experiments. Unregulated F-actin filament motility was measured at 30°C. Experimental procedures were as previously described (Razumova *et al.* 2006). At least six unique areas of each assay chamber were recorded for 10 s each at 10 Hz. Recordings were analysed digitally, using custom software developed in house. The criteria for inclusion/exclusion of filaments and additional information on this method are detailed in the statistics section below, and in previous publications (Homsher *et al.* 1992; Racca *et al.* 2013).

Contractile protein isoform composition. To determine MHC isoform composition, samples were dissected from the left ventricles utilized in the functional studies and prepared for SDS-PAGE. Briefly, left ventricle tissue was homogenized in CellLytic (Sigma), with the addition of protease inhibitors, using a glass mortar and pestle chilled on ice. Protein concentrations were determined using a Bradford assay (Bio-Rad Laboratories, Hercules, CA, USA). The myosin isoforms in these samples were separated as previously described (Van Hees *et al.* 2007) using a Mini-PROTEAN Tetra Cell (Bio-Rad Laboratories). The stacking gel was 4% acrylamide (pH 6.8) and the separating gel contained 7% acrylamide (pH 8.8) with 30% (v/v) glycerol. Gels were run for ~16 h at 4°C. Gels were then stained with SYPRO Ruby (Molecular Probes) following the manufacturer's instructions and imaged using a BioSpectrum Imaging System (UVP, Upland, CA, USA).

To determine the contractile protein isoform composition in human fetal left ventricle muscle SDS-PAGE and Western blotting was used. In brief, human fetal and adult left ventricle samples were separated on 10% or 12% SDS-PAGE gels using a Mini-PROTEAN Tetra Cell (Bio-Rad Laboratories). The

SDS-PAGE gel was transferred onto a polyvinylidene fluoride (PVDF) membrane using the Mini-PROTEAN Tetra Cell wet transfer system (Bio-Rad Laboratories). The primary antibodies used were as follows: cTnI (sc-15368, Santa Cruz Biotechnology, Santa Cruz, CA, USA), ssTnI (sc8119, Santa Cruz), cTnT (sc8121, Santa Cruz), GAPDH (Rockland Immunochemicals, Gilbertsville, PA, USA); and the α-MHC (BAG5) and β-MHC were a gift from Charles Murry (University of Washington). There were two to five technical replicates for each sample, and two biological replicates (two separate fetal hearts aged 130 days). Images were analysed using ImageJ software (National Institutes of Health, Bethesda, MD, USA). Troponin expression was first standardized to GAPDH and the expression levels were normalized to the 134-day-old sample.

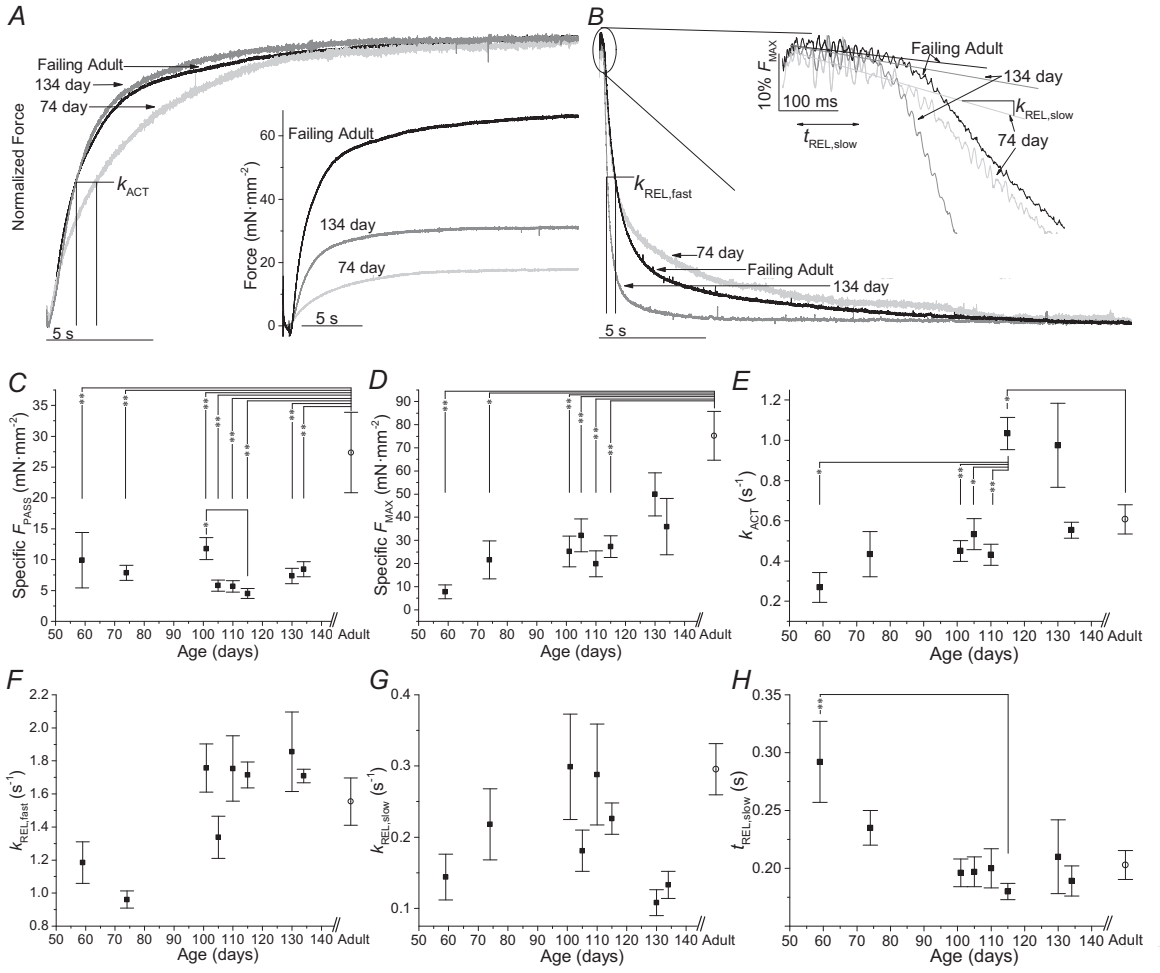

Figure 1. Human fetal left ventricle myofibril kinetics from 55 to 134 days of gestation
A and *B*, representative myofibril force traces for human fetal left ventricle myofibrils at 74 days of gestation (light grey) and 134 days of gestation (dark grey) and human adult stage IV heart failure left ventricle myofibrils (black). *A*, activation traces showing activation kinetic differences between human fetal left ventricle myofibrils at 74 and 134 days of gestation and adult left ventricle myofibrils; *y*-axis is force normalized to each myofibril's specific force at maximal calcium concentration (F_{MAX}); bar shows 5s. Inset, activation trace showing magnitude of activation; vertical bar shows 10 mN mm^{-2}; horizontal bar shows 5 s. *B*, relaxation traces showing relaxation kinetic differences between human fetal left ventricle myofibrils at 74 and 134 days of gestation and adult left ventricle myofibrils; *y*-axis is force normalized to each myofibril's specific force at maximal calcium concentration (F_{MAX}); bar shows 5 s. Inset, close-up of the slow phase of relaxation of the myofibrils (bold lines), in response to a change from maximum [Ca^{2+}] (*p*Ca 4.0) to minimum [Ca^{2+}] (*p*Ca 9.0), showing slow phase kinetics; vertical bar shows 10% F_{max}; horizontal bar shows 100 ms. Straight lines indicate the slow phase fit ($k_{REL,slow}$); bold lines indicate data considered part of the slow phase; thin lines indicate the total normalized relaxation data. *C–H*, changes in the kinetics and force of fetal left ventricle myofibrils grouped by the age of gestation, compared to human adult. *C*, specific passive force in relaxing solution (F_{PASS}); *D*, specific force production at maximum concentration of calcium (F_{MAX}); *E*, the rate of activation (k_{ACT}); *F*, the duration of the slow phase of relaxation ($t_{REL,slow}$); *G*, the rate of the slow phase of relaxation ($k_{REL,slow}$); *H*, the rate of the fast phase of relaxation ($k_{REL,fast}$).

Electron microscopy imaging. For ultrastructural determination, same-day dissected tissues from human fetal heart muscle of three different fetuses (at 52, 108 and 127 days of gestation) were fixed in 4% glutaraldehyde and stored at 4°C until processing. The tissues were then post-fixed in osmium tetroxide, dehydrated with ethanol and embedded in Poly/Bed 812 epoxy resin. Ultrathin longitudinal sections were stained with lead citrate and viewed and photographed on a JEOL 1230 transmission electron microscope (Jeol USA Inc., Peabody, MA, USA). Images were analysed using ImageJ software (National Institutes of Health).

Statistics

Myofibril experiments. All values in Tables 2 and 3 are reported as means ± SEM. The number of fibrils (n) in each mean is also reported, as well as the number of fetuses or adult samples (N). A one-way ANOVA with a Tukey *post-hoc* test was used to compare between myofibril groups with statistical significance set at $P < 0.05$.

***In vitro* motility.** Mean speed and error of mean speed were weighted according to the duration of the filament trace and the number of filaments per slide (Racca *et al.* 2013) and are described briefly below.

Using a previously described filtering technique (the Homsher–Sellers ratio), in which a ratio of mean to SD of velocity was used to eliminate erratically moving filaments, the optimal ratio for this study (0.6) was determined by analysing recordings with a motility solution [ATP] = 2 mM. Filaments that moved erratically were not included in the analysis. Erratic filaments stalled, crossed paths with another filament, crossed themselves or pulled apart into separate pieces.

Additional statistical analysis was performed on *in vitro* motility data to propagate uncertainties associated with filament speeds. This statistical analysis was based on prior reporting (Homsher *et al.* 1992; Clemmens & Regnier, 2004; Racca *et al.* 2013). Filament mean speeds (u) and standard deviations (σ) were weighted according to the number of frames a filament was present and the number of filaments recorded, using eqn (1):

$$\bar{u} = \sum \left(u_i * \frac{w_i}{\sum w_i} \right); \; \sigma = \sqrt[2]{\sum \sigma_i * \left(\frac{w_i}{\sum w_i} \right)^2} \quad (1)$$

Results

Study populations

Overall 17 human fetus samples were acquired for this project, with the greatest number ($N = 10$) being between 101 and 116 days of gestation. Samples outside this age range were rare due to regulatory limits (illegal at > 24 weeks, 168 days of gestation) and alternative procedures available (Mifeprex for < 9 weeks, 63 days of gestation). Table 1 describes the age, sex, reported ethnicity and which experiments each sample was used for. Two samples were acquired at 130 days of gestation for myofibril experiments, one at 127 days of gestation for electron microscopy analysis only, and one at 134 days of gestation for use in myofibril and *in vitro* motility assays. One fetal heart sample was collected from a 52 day fetus, but it did not produce functional myofibrils, so it was used only for electron microscopy imaging. The other two younger age fetal samples were at 59 and 74 days of gestation, and both were used for myofibril experiments only. These samples are typically small and fragile, especially with respect to those < 100 days of gestation. As such, very few functional myofibrils were obtained from the younger ages. Samples that were within 3 days of each other were pooled for myofibril analysis in an effort to improve statistical power, although generating statistically significant differences in these samples was still a challenge. Therefore, the results presented below should not be considered definitive until additional studies can confirm them. Additionally, because we were limited in the tissue we could obtain, we chose to prioritize measurements of the contractile properties for the current study, and used additional available tissue for limited protein and structural analysis.

For comparison with human fetal samples, human adult samples were collected from eight patients who were enrolled in the study. Six out of eight patients (75%) were males and the average age of the cohort was 48 ± 15 years (24–67 years). The etiology of heart failure in all patients used in the study was non-ischaemic. Details for this patient population have been reported previously (Moussavi-Harami *et al.* 2015).

Myofibril passive force and sarcomere length

Myofibrils were stretched to 110% slack length. If sarcomeres were visible, which was the case for a majority of the myofibrils, the sarcomere length at this stretch was recorded, and on average, was shown to be ~2.3 μm per sarcomere. Before activation, passive force was measured. The average specific passive force (F_{PASS}) varied greatly between the fetal ages (Table 2). F_{PASS} was highest at 101 days (12.5 ± 1.8 mN mm^{-2}; $n = 11$), and lowest at 114–116 days mN mm^{-2} (4.0 ± 0.7 mN mm^{-2}; $n = 38$) ($P < 0.05$ between these two groups) (Fig. 1*C*). This variation did not appear to be a function of the average width of the preparations (4.7–7.2 μm, Table 2). Overall, F_{PASS} was much lower than what is seen for adult stage IV heart failure ventricle samples (27 ± 7 mN mm^{-2}; $n = 8$; Table 2) ($P < 0.01$ *vs.* all fetal groups).

Table 2. F_{MAX} and kinetic parameters for maximum [Ca^{2+}] activation (*p*Ca 4.0) and relaxation of fetal myofibrils *vs.* adult myofibrils from stage IV heart failure patients' left ventricles at 15°C

			Activation		Relaxation				
					Slow		Fast		
Parameter (units)	Avg. width (μm)	Specific F_{PASS} (mN mm^{-2})	Specific F_{MAX} (mN mm^{-2})	k_{ACT} (s^{-1})	$t_{REL,slow}$ (s)	$k_{REL,slow}$ (s^{-1})	$k_{REL,fast}$ (s^{-1})	$t_{REL,50}$ (s)	$t_{REL,90}$ (s)
59 days ($N = 1$)	7.0 ± 2.9 (4)	9.9 ± 4.5 (4)^{A}	7.8 ± 3.0 (3)^{a}	0.27 ± 0.07 (4)^{a}	0.292 ± 0.035 (4)^{A}	0.14 ± 0.03 (3)	1.18 ± 0.13 (2)	0.59 ± 0.06 (2)	15.5 ± 2.0(3)^{A,b}
74 days ($N = 1$)	6.1 ± 1.4 (5)	7.9 ± 1.2 (5)^{B}	23.1 ± 8.3 (5)^{b}	0.43 ± 0.12 (5)	0.235 ± 0.015 (5)	0.22 ± 0.05 (5)	0.96 ± 0.05 (5)	0.73 ± 0.05 (5)^{a}	14.4 ± 3.1 (5)^{C,D}
101 days ($N = 1$)	4.8 ± 1.2 (12)	12.5 ± 1.8 (11)^{C,i}	25.2 ± 6.6 (11)^{C}	0.45 ± 0.05 (11)^{B}	0.192 ± 0.013 (11)	0.32 ± 0.08 (11)	1.84 ± 0.13 (12)	0.40 ± 0.03 (12)^{a}	7.3 ± 2.1 (9)
105–107 days ($N = 2$)	7.2 ± 0.7 (12)	7.0 ± 1.6 (12)^{D}	36.9 ± 10.6 (13)^{D}	0.57 ± 0.12 (13)^{c}	0.198 ± 0.015 (13)	0.20 ± 0.05 (11)	1.36 ± 0.18 (13)	0.60 ± 0.06 (13)	12.0 ± 1.6 (13)^{E,F}
110 days ($N = 2$)	5.2 ± 0.7 (12)	5.7 ± 0.9 (12)^{E}	19.9 ± 5.6 (12)^{e}	0.43 ± 0.05 (12)^{D}	0.200 ± 0.017 (12)	0.29 ± 0.07 (12)	1.75 ± 0.20 (12)	0.45 ± 0.05 (12)	8.0 ± 1.5 (12)
114–116 days ($N = 3$)	5.2 ± 0.4 (40)	4.0 ± 0.7 (38)^{F,i}	26.9 ± 4.8 (39)^{f}	1.04 ± 0.08 (38)^{a,B,c,D,E}	0.180 ± 0.007 (39)^{A}	0.23 ± 0.02 (39)	1.68 ± 0.08 (40)	0.47 ± 0.03 (40)	5.1 ± 0.8 (37)^{b,D,F}
130 days ($N = 2$)	4.7 ± 0.8 (8)	7.4 ± 1.2 (8)^{G}	49.9 ± 9.3 (8)	0.98 ± 0.21 (8)	0.210 ± 0.032 (8)	0.11 ± 0.02 (8)	1.86 ± 0.24 (7)	0.42 ± 0.06 (7)	7.2 ± 2.3 (7)
134 days ($N = 1$)	5.3 ± 1.1 (4)	8.4 ± 1.2 (4)^{H}	36.0 ± 12.1 (4)	0.55 ± 0.04 (4)	0.189 ± 0.013 (4)	0.13 ± 0.02 (4)	1.71 ± 0.04 (4)	0.41 ± 0.01 (4)	5.3 ± 2.7 (4)
Adult ($N = 8$)	5.9 ± 0.8 (8)	27.4 ± 6.5 (8)$^{A–H}$	75.2 ± 10.6 (19)^{a,b,C,d,E,F}	0.61 ± 0.07 (16)^{E}	0.203 ± 0.012 (21)	0.30 ± 0.04 (19)	1.55 ± 0.14 (21)	0.52 ± 0.04 (21)	3.5 ± 0.6 (15)^{A,C,E}

A one-way ANOVA between all nine groups with a Tukey *post-hoc* test was used to determine statistical significance. Lower case letters denote a significant difference of $P < 0.05$. Upper case letters denote a significant difference of $P < 0.01$. Significant differences are indicated by the same superscript letter, within columns. Data are mean ± SEM, *N* indicates the number of separate fetal or adult samples and numbers in parentheses represent the number of myofibrils.

Table 3. F_{MAX} and kinetic parameters for submaximal [Ca^{2+}] activation (*p*Ca 5.8) and relaxation of fetal myofibrils at 15°C

Parameter (units)	Specific $F_{pCa5.8}$ (mN mm^{-2})	% of F_{MAX}	k_{ACT} (s^{-1})	$t_{REL,slow}$ (s)	$k_{REL,slow}$ (s^{-1})	$k_{REL,fast}$ (s^{-1})
74 days ($N = 1$)	17.5 ± 5.6 (5)	87 ± 29 (5)	0.34 ± 0.07 (4)	0.211 ± 0.034 (4)	0.30 ± 0.08 (4)	1.15 ± 0.17 (5)
115 days ($N = 1$)	27.2 ± 5.6 (18)	74 ± 5 (16)	0.61 ± 0.08 (18)	0.142 ± 0.011 (18)	0.35 ± 0.04 (18)	2.11 ± 0.18 (18)
134 days ($N = 1$)	26.4 ± 3.5 (3)	62 ± 12 (3)	0.40 ± 0.11 (3)	0.142 ± 0.041 (3)	0.40 ± 0.24 (2)	2.26 ± 0.71 (2)

Data are mean ± SEM, *N* indicates the number of separate fetal samples at a particular age and numbers in parentheses represent the number of myofibrils. The % of F_{MAX} is calculated as $F_{pCa5.8}/F_{pCa4.0}$ for each myofibril.

Myofibril activation and relaxation kinetics

Myofibrils were exposed to rapid solution switching for step increases and decreases in Ca^{2+}, from *p*Ca 9.0 to 4.0 and back to 9.0 (see Methods), to determine the magnitude and rate of force generation and relaxation at 15°C. Representative myofibril force traces from 74 and 130 days of gestation fetal tissue samples and one from adult stage IV heart failure sample are shown in Fig. 1 for activation and relaxation. These traces demonstrate that the 74 day myofibrils produce much less force (Fig. 1*A*, inset) and have a slower rate of force development (Fig. 1*A*) and relaxation (Fig. 1*B*) than 134 day fetal and adult stage IV heart failure myofibrils. The data for all the fetal and adult myofibrils are summarized in Fig. 1(*C–H*) and quantitative values are reported in Table 2. The average width of the preparations varied by as much as 35%. We normalized the active maximal force per myofibril bundle to the width of the bundle, yielding maximal specific force, and fetal myofibrils produced progressively more maximal specific force (F_{MAX}) as they aged. F_{MAX} at 59 days (7.8 ± 3.0 mN mm^{-2}; $n = 3$) was one-third of the force produced at 74 days (23.1 ± 8.3 mN mm^{-2}; $n = 5$) and 101 days of gestation (25.2 ± 6.6 mN mm^{-2}; $n = 11$). At 105–107 days of gestation (36.9 ± 10.6 mN mm^{-2}; $n = 13$) and 114–116 days of gestation (26.9 ± 4.8 mN mm^{-2}; $n = 39$) F_{MAX} was three- to four-fold higher compared with the 59 days of gestation value. At 130 days of gestation F_{MAX} (49.9 ± 9.3 mN mm^{-2}; $n = 8$) increased further, being six-fold greater than the 59 day values. However, even at 130 and 134 days of gestation, F_{MAX} was still considerably less than that of adult left ventricle samples from either stage IV heart failure patients (75.2 ± 10.6 mN mm^{-2}) or presumed healthy controls as reported by others (90–110 mN mm^{-2}; Piroddi *et al.* 2007; Belus *et al.* 2008).

The rate of force production (k_{ACT}; Fig. 1*A*, *E* and Table 2) represents the processes of Ca^{2+}-dependent thin filament activation, myosin cross-bridge binding and force production. k_{ACT} for fetal myofibrils increased progressively as myofibrils aged (Table 2). Compared with 59 days (0.27 ± 0.07 s^{-1}; $n = 4$), k_{ACT} increased 60% by 74–107 days of gestation, and had tripled by 114–116 days (1.04 ± 0.08 s^{-1}; $n = 38$), $P < 0.05$ *vs.* 59 days) of gestation. For the two samples of 130 days of gestation, k_{ACT} was still considerably higher (0.98 ± 0.21 s^{-1}; $n = 8$) compared with the sample of 59 days of gestation, although with the low number of myofibrils from limited samples, this was not statistically significant. The 134 day sample was much slower to activate than both of the 130 day samples, but this may an artifact of sample collection and/or handling given that the single sample provided only four functional myofibrils, and these myofibrils also produced less force (36.0 ± 12.1 mN mm^{-2}; $n = 4$) than the myofibrils at 130 days of gestation. At days 114–116, myofibrils from fetal ventricle samples produced force at a faster rate than those from adult stage IV heart failure ventricle samples (0.61 ± 0.07 s^{-1}; $n = 16$; $P < 0.05$ *vs.* 114–116 days) and what has been reported by others from presumed healthy control adult ventricle tissue (0.73–0.84 s^{-1}; Piroddi *et al.* 2007; Belus *et al.* 2008). They also produced force at a slower rate than that reported for presumed healthy control adult atrial tissue (~3.7 s^{-1}; Piroddi *et al.* 2007; Belus *et al.* 2008).

Fetal cardiac myofibril relaxation also increased in speed with age, as described by the time to 50% ($t_{REL,50}$). At 59 days (0.59 ± 0.06 s; $n = 2$) and 74 days (0.73 ± 0.05 s; $n = 5$), myofibrils were relaxing more than 50% slower than at 101 days (0.40 ± 0.03 s; $n = 12$; $P < 0.05$ *vs.* 74 days) and older. This was even more pronounced by the time to 90% relaxation ($t_{REL,90}$), which gradually decreased as myofibrils aged from 59 days (15.5 ± 2.0 s; $n = 3$) to nearly half that time at 101 days (7.3 ± 2.1 s; $n = 9$), and one-third of the time by 114–116 days (5.1 ± 0.8 s; $n = 37$; $P < 0.05$ *vs.* 59 days). The time to 90% relaxation was prolonged in all the fetal samples compared with the adult stage IV heart failure samples (3.5 ± 0.6 s; $n = 15$). This difference in relaxation speed is shown in Fig. 1*B*, which compares example myofibril traces in adult sage IV heart failure and at 74 and 130 days of gestation and summarized in Table 2.

Force relaxation in myofibrils is characterized by an initial slow ($k_{REL,slow}$, $t_{REL,slow}$; Fig. 1*B*, inset) and secondary fast ($k_{REL,fast}$; Fig. 1*B*) phase. $k_{REL,fast}$ is thought to reflect the phenomenon of sarcomere give, in which uneven sarcomere lengths during relaxation create more strain on nearby sarcomeres, causing a propagation of sarcomere

release (Poggesi *et al.* 2005), and may be independent of the Ca^{2+} sensitivity of the myofilament (De Tombe *et al.* 2007). Compared with 59 days ($1.18 \pm 0.13\ s^{-1}$; $n = 2$) and 74 days ($0.96 \pm 0.05\ s^{-1}$; $n = 5$), $k_{REL,fast}$ was ~50% faster for 101–134 day samples (Fig. 1*F*; Table 2). However, even at 130 days myofibrils from the fetal heart ventricle samples relaxed at rates about 20% greater ($1.86 \pm 0.24\ s^{-1}$; $n = 7$) than those from adult stage IV heart failure left ventricle ($1.55 \pm 0.14\ s^{-1}$; $n = 21$) and at much slower rate compared with the reported values by others for presumed healthy control adult ventricle (~$2.9\ s^{-1}$) and atrial (~$16.0\ s^{-1}$) tissue (Piroddi *et al.* 2007; Belus *et al.* 2008).

The early, slow phase rate of relaxation, $k_{REL,slow}$, is thought to be determined by the rate of cross-bridge detachment during maximal Ca^{2+} activation (Tesi *et al.* 2002). In contrast to $k_{REL,fast}$, $k_{REL,slow}$ (Fig. 1*G*) increased progressively from 59 days ($0.14 \pm 0.03\ s^{-1}$; $n = 3$) to 74 days ($0.22 \pm 0.05\ s^{-1}$; $n = 5$) and 101 days ($0.32 \pm 0.08\ s^{-1}$; $n = 11$). It appeared to decrease again with the 130 day samples ($0.11 \pm 0.02\ s^{-1}$; $n = 8$). At 101 and 110 days, the $k_{REL,slow}$ values are closer to those seen in adult stage IV heart failure ventricle samples ($0.30 \pm 0.04\ s^{-1}$; $n = 19$). Interestingly, $k_{REL,slow}$ for presumed healthy control human adult ventricle was reported to be 0.15–$0.17\ s^{-1}$, half of what we report at 101 days and in our stage IV heart failure adult samples, but close to what we report at 59 and 130–134 days, while the human adult atria $k_{REL,slow}$ is reported to be faster (~$0.52\ s^{-1}$; Piroddi *et al.* 2007; Belus *et al.* 2008).

We have previously reported that the slow phase duration ($t_{REL,slow}$) may be influenced by the properties of thin filament regulatory proteins and the level of Ca^{2+} activation (Kreutziger *et al.* 2008, 2011). There was a 35% decrease in $t_{REL,slow}$, from 59 days (0.292 ± 0.035 s; $n = 4$) to 101 days (0.192 ± 0.013 s; $n = 11$) and it remained around 200 ms at later time points out to 134 days. However, outside of the initial time point at 59 days *vs.* 114–116 days (0.180 ± 0.007 s; $n = 39$), the other prenatal time points for $t_{REL,slow}$ do not differ significantly from one another. The duration of the slow phase for older fetal tissues was close to what we found in adult stage IV heart failure left ventricle tissues (0.203 ± 0.012 s; $n = 21$). These older fetal ventricle values are slower than what has been reported for control human adult ventricles at *p*Ca 4.0 by others (0.225–0.226 s), and faster than what is seen in human adult atria myofibrils (~0.126 s) (Piroddi *et al.* 2007; Belus *et al.* 2008).

We also activated a subset of myofibrils of different gestational ages at a submaximal concentration of calcium (*p*Ca 5.8; Table 3) to examine possible changes in calcium sensitivity. To avoid bias due to run-down of the myofibrils, half of the myofibrils were first activated at *p*Ca 5.8, then following relaxation, activated at *p*Ca 4.0. This order was reversed for the other half of the myofibrils. The force production at this submaximal calcium appeared to decrease with age, suggesting a decrease in calcium sensitivity as the fetal heart ages from 74 to 134 days of gestation. At 74 days, the force produced at *p*Ca 5.8 was 87% of the force produced at maximum calcium concentration (*p*Ca 4.0). At 114–116 days, *p*Ca 5.8 produced only 74% of maximum force, and by 134 days of gestation this was reduced to only 62% of the force produced at *p*Ca 4.0, indicating fetal heart ventricle myofibrils have elevated calcium sensitivity compared with adult ventricle myofibrils. In addition to a higher calcium sensitivity, fetal ventricle myofibril activation rates at *p*Ca 5.8 were 95% (74 days), 74% (115 days) and 71% (134 days) of the activation rates of the same myofibrils at *p*Ca 4.0. These results suggest there may be a gradual decrease in the calcium sensitivity of myofibril contraction. Finally, the duration of the slow phase of relaxation following activation at *p*Ca 5.8 was 94% (74 days), 83% (115 days) and 79% (134 days) the duration of the same myofibril following activation at *p*Ca 4.0 (Table 3). This decrease in the slow phase of relaxation may indicate a change in Ca^{2+} release rate of troponin is altered throughout gestation.

Fetal cardiac myosin sliding velocities

The slow activation and relaxation kinetics of fetal myofibrils (compared with adult myofibrils) suggested much slower fetal myosin cross-bridge cycling and ATPase activity. To investigate this we measured sliding velocity of F-actin (V_f) propelled by HMM prepared from fetal human left ventricle tissue of three fetuses (101, 116 and 134 days of gestation) in the *in vitro* motility assay, where myosin–actin interactions can be measured in the absence

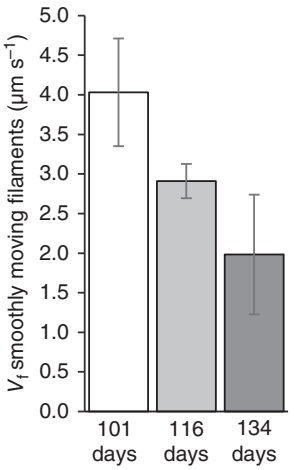

Figure 2. Unregulated F-actin filament sliding velocity of fetal human left ventricle decreases with age
The speed of smoothly moving actin filaments (V_{MAX}) over fetal human left ventricle heavy meromyosin from 101, 116 and 134 days of gestation. Data shown are as weighted mean and weighted SD.

of regulatory proteins and at a temperature that is closer to physiological than can be used in myofibril mechanical assays. Maximal sliding velocity (V_{MAX}, measured at 30°C) for fetal HMM at 101 days was 4.03 ± 0.62 μm s^{-1}, almost two-fold faster than V_{MAX} at 134 days (1.98 ± 0.76 μm s^{-1}). This was consistent with faster $k_{REL,slow}$ at ∼100 *vs.* 134 days, and suggests myosin cycling and cross-bridge detachment may decrease over this time period (Fig. 2).

Contractile protein expression

Human fetal left ventricle contained both ssTnI and cTnI protein isoforms as confirmed by Western blot (Fig. 3*A*). We observed a progressive increase in the relative proportion of cTnI to the total amount of TnI present as the fetal heart aged, in agreement with others (Sasse *et al.* 1993), and its increase in density was similar to what was seen for the total amount of troponin T (Fig. 3*B*, *C*). Using both the C-19 and the mAB13-11 cardiac TnT antibodies, we detected a total of three bands in fetal cardiac tissue and two in the adult failing left ventricle, consistent with Anderson *et al.* (1991) (Fig. 3*B*). However, in the current study there was a clear predominant TnT isoform (TnT3) in the fetal left ventricle and the other two isoforms detected were of low abundance. Troponin density (Fig. 3, normalized to GAPDH) indicated an increase in protein density within the tissue as a function of fetal age. We found β-MHC expressed in human fetal left ventricle and adult ventricle samples (Fig. 4) at all ages, with little to no expression of α-MHC, which is consistent with reports by others (Reiser *et al.* 2001) of only ∼0–3% α-MHC at ∼110 days of gestation. To confirm that no α-MHC was present, we used a tissue sample of rat atria and ventricle, which demonstrates that α-MHC is present in the rat atria and ventricle, but not visible in the human fetal or adult ventricle samples.

Electron microscopy and ultrastructure of fetal left ventricle muscle

To elucidate the potential influence of structure on the functional changes in these fetal tissues, sections of left ventricle from 52, 108 and 127 days of gestation were imaged using electron microscopy (Fig. 5). The small size of the samples meant that it was not possible to use the same sample for imaging and mechanical analysis. Because pre-treatment was not possible, these samples were fixed in varying states of contraction; most notably, the 108 day sample appears to be fully contracted, while the 52 day sample appears to be relaxed. We therefore focused on features, such as the widths of the myofibrils and structure of the contractile apparatus, that would build on previous observations (Kim *et al.* 1992). Within the myofibrils at day 52, z-bands were crooked and did not align between adjacent myofibrils, myofibrils were very narrow in width at the Z-band (0.36 ± 0.02 μm; n = 90) and the muscle had low myofibril density (Fig. 5*A*). Correlating with a doubling in force production (Fig. 1*C*), by day 108 Z-bands were straight, aligned

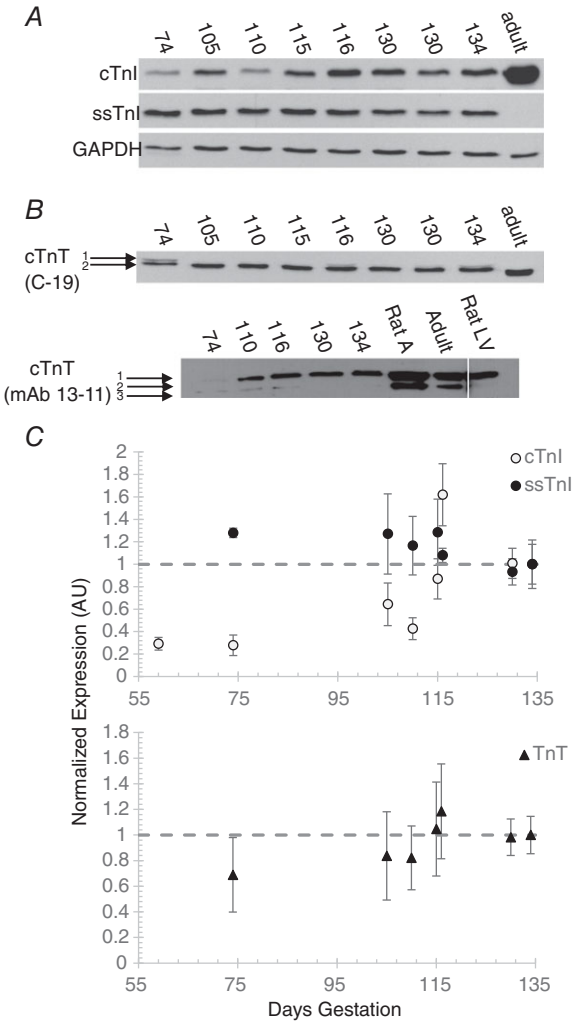

Figure 3. Troponin I and troponin T expression in human fetal left ventricles
A, Representative Western blot of cardiac troponin I (cTnI), slow skeletal troponin I (ssTnI) and a loading control GAPDH from human fetal left ventricles between the ages of 74 and 134 days of gestation and adult failing left ventricle (Adult). *B*, representative Western blot of cardiac TnT expression in human fetal left ventricles using both a C-19 and mAb13-11 antibodies (top and bottom panel, respectively); Adult – adult failing left ventricle, Rat LV – adult rat left ventricle, Rat A – adult rat atrium. *C*, normalized expression of troponin across the age range of fetal ventricle samples. Top panel shows normalized expression of cTnI and ssTnI, bottom panel normalized expression of TnT (calculated from the predominant isoform, labelled 2, from the C-19 Western blots). Data are mean ± SEM; there were two to five technical replicates for each sample, and two biological replicates (two separate fetal hearts aged 130 days). Troponin expression was first standardized to GAPDH and the expression levels were normalized to the 134 day sample.

across adjacent myofibrils, and myofibrils were noticeably wider (0.457 ± 0.01 μm; $n = 297$) (Fig. 5*B*). Finally, at day 127, the muscle had greater myofibril density and myofibril width approximately doubled from day 108 (0.97 ± 0.02 μm; $n = 427$) (Fig. 5*C*). At all three ages we observed the thick filament (H zone) region was often not distinct, consistent with previous observations (Kim *et al.* 1992). However, our ability to study this in detail was limited, due to the small amount of tissue available for these measurements and to some inconsistency in the time between tissue harvesting and fixation that was unavoidable.

Discussion

Here we report for the first time changes in the contractile properties of human fetal cardiac muscle during 59–134 days of gestation and compare them with human adult stage IV heart failure muscle. We characterized several kinetic parameters of contraction and relaxation that are altered during the maturation of the fetal heart which correlate with changes in sarcomeric protein isoforms and maturation of sarcomere structure and myofibril organization within cardiomyocytes.

Force production

The force produced by human fetal left ventricle myofibrils increases considerably as the fetal heart ages (Fig. 1 and Table 2). However, even at 130–134 days of gestation, the fetal left ventricle myofibrils still produced considerably less specific force than our stage IV heart failure human adult ventricle myofibrils and less than half the specific force previously reported for presumed healthy adult ventricle myofibrils (Piroddi *et al.* 2007). There are at least two potential explanations for the gain in force production from 59 to 134 days of gestation. (1) The ultrastructure of the fetal cardiac myofibrils undergoes significant development and remodeling; in particular the width and alignment of z-discs increases and the overall width of myofibrils increases. This allows more force to be translated along the sarcomeres and the myofibril. In the small bundles used for mechanical measurements, the older bundles contain more sarcomeres that are aligned and allow force to be translated laterally. (2) Myosin density within the sarcomere increases, increasing the number of cross-bridge bindings and thus force generating capacity.

We have previously reported that human fetal skeletal muscle ultrastructure is underdeveloped at 108 days of gestation (Racca *et al.* 2013). In addition, Kim *et al.* (1992) demonstrated that later term human fetal hearts, at 119 days of gestation, had myofibrils that were short, loosely packed and lacking consistently definitive Z-bands. In the current study, we found that cardiac muscle ultrastructure also lacks order at 52, 108 and 127 days of gestation, although there are considerable increases in the width and alignment of myofibril z-discs between these time points. These results are consistent with studies on the ultrastructure of fetal lamb and guinea pig, which showed that as the fetal heart ages myofibril density of cells increases, elongation and alignment of neighbouring myofibrils increase, and myofibrils widen in diameter (Sheldon *et al.* 1976; Rolph *et al.* 1982). We are unable to address changes in sarcomere length due to our inability to pre-treat samples prior to placement in the electron microscopy buffer. The lack of order in the structure of the myofibril can at least partially explain the low force production compared with adult myofibrils, as transmission of strain generated by myosins may be less efficient. This effect could be compounded by differences in the series elastic components of sarcomeres. Moreover, as the myofibril ultrastructure develops between 59 and 134 days of gestation the longer and wider myofibrils would have increased acto-myosin interaction. This change in ultrastructure probably contributes to the increase in force and some of the increases in the kinetics of activation and relaxation throughout gestation. Finally, the possibility that the myofibril bundles contain non-aligned or non-sarcomeric tissue cannot be excluded, as the electron microscopy images indicate that sections of laterally joined myofibrils are thin, especially in the younger aged myofibrils, and while the preparations were chemically skinned with both glycerol and Triton, some non-sarcomeric tissue may remain.

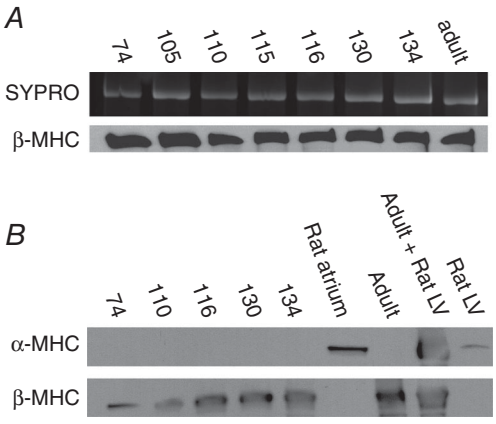

Figure 4. Myosin heavy chain expression in human fetal left ventricles
A, SYPRO ruby stain for total protein (top panel) and Western blot (bottom panel) showing β myosin heavy chain (MHC) expression in fetal left ventricle samples across the range 74–134 days of gestation. MHC was separated using 7% acrylamide and 30% glycerol gels (Van Hees *et al.* 2007). *B*, Western blot for α-MHC (top panel) and β-MHC (bottom panel) in a subset of fetal left ventricle samples. Rat left ventricle and atrium were used as a control for α-MHC and proteins were separated using a 10% acrylamide gel. Adult – failing adult left ventricle, Rat LV – adult rat left ventricle.

Studies in fetal mice report that the overall increase in myosin density is a key player in an age-correlated increase in force production (Siedner *et al.* 2003). In the current study, we were unable to show a change in myosin density within the age range examined, but we report a small increase in overall TnI and TnT density. As the overall density of the contractile proteins can change as a result of either an increase in the number of myofibrils or an increase in the size of the myofibrils within a cell, both of which are shown to occur with the electron microscopy work (Fig. 5). Together, the increase in troponin density per cell (Fig. 3) and the increase in myofibrils seen by electron microscopy (Fig. 5) suggest an overall increase in myofibril protein density per cell and lend more support to the idea that ultrastructural maturation plays a key role in increasing force production in the developing human fetal heart.

Kinetics of activation and relaxation

We have reported here that the activation and relaxation kinetics of myofibrils from human fetal left ventricle increase in speed as the fetal heart ages. At 130–134 days of gestation relaxation is faster than our adult stage IV heart failure ventricle samples, but significantly slower than what has been reported for a control population of adult ventricle myofibrils (Piroddi *et al.* 2007). This is the case even though the predominant myosin isoform expressed is β-MHC at all time points (Fig. 4*B*).

One likely mechanism for the increase in activation and relaxation kinetics is that the ultrastructure development between 59 and ∼100 days of gestation allows for better Z-disc and sarcomere alignment within the small bundles of myofibrils used in our experiments, which may decrease compliance and cause strain to translate across the myofibril more efficiently (Martyn *et al.* 2002). This may affect the kinetics of force development even more than the magnitude. Additionally the thick and thin filaments are more tightly bundled, which could increase the interaction efficiency of myosin and actin (Williams *et al.* 2010, 2013). This increase in ultrastructural order could also be responsible for variation in cross-bridge detachment rates seen in the myofibril slow phase (Figs 1*G* and 5); the overall myosin density may increase during this period and reach a critical density where the myosin and actin can better interact. However, we could not study this with the limited number and quality of samples available for structure and protein analysis. Also, changes in myosin or troponin proteins (from ssTnI to cTnI) cannot be ruled out as having influence on the changing kinetics of the human fetal heart as it develops.

The data from the myofibril $k_{REL,slow}$ measurements and the maximum velocity of unregulated actin filament sliding (V_{MAX}) in the *in vitro* motility assay suggest

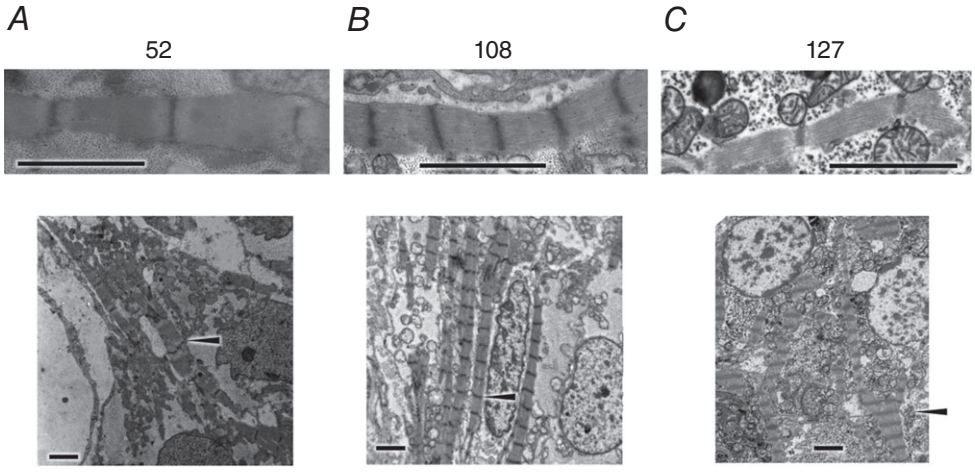

Figure 5. Ultrastructural assessment of human fetal left ventricle
Transmission electron micrographs of left ventricle sections from three fetal hearts at 52, 108 and 127 days of gestation. All scale bars are 2 μm. *A*, top, 52 day left ventricle appears to be relaxed, with longer sarcomere length, and shows thick filament presence and thin myofibrils (average width ∼0.36 ± 0.02 μm; $n = 90$). *A*, bottom, 52 day left ventricle shows poor z-disc alignment between myofibrils, wavy z-discs within myofibrils (arrow) and low myofibril density. *B*, top, 108 day left ventricle appears to be in a contacted state with very short sarcomere lengths, and shows definitive m-line within sarcomeres. *B*, bottom, 108 day left ventricle shows medium myofibril density and z-disc alignment between adjacent myofibril (arrow). Average width of segment of myofibrils is ∼0.457 ± 0.01 μm ($n = 297$). *C*, top, 127 day left ventricle appears to be relaxed with long sarcomere lengths, and shows definitive m-line within sarcomeres. *C*, bottom, 127 day left ventricle shows high myofibril density and z-disc alignment between adjacent myofibril (arrow), as well as larger myofibril widths overall (average width ∼0.97 ± 0.02 μm; $n = 427$).

cross-bridge detachment rate slows considerably between ~100 and ~130 days of gestation. This is the opposite of what we might have expected due to the increase in contractile kinetics in myofibrils. V_{MAX} with myosin from the 101 and 116 day fetal left ventricle was much slower than we have shown for adult fast skeletal myosin (gene *MYH2*; Racca *et al.* 2013) and myosin from rat hearts (Regnier *et al.* 2000), but faster than speeds reported from adult human myosin (Moussavi-Harami *et al.* 2015). The V_{MAX} of the myosin from the 134 day sample was similar to that reported for myosin from adult human (Moussavi-Harami *et al.* 2015). We found that $k_{REL,slow}$ of adult stage IV heart failure myofibrils is comparable to that of fetal samples at 101 days, and faster than that of fetal samples at 130–134 days. One potential explanation for these changes in cross-bridge cycling kinetics is a change in the MHC isoform expressed. However, in the current study, we were only able to detect β-MHC in the fetal and adult ventricle samples using both Western blots and SYPRO staining. In contrast, previous work has shown that the human fetal left ventricle contains a small amount of α-MHC (<5%) and that there is a significant reduction in α-MHC from 47 to 100 days of gestation (Reiser *et al.* 2001). However, in a study by Krenz *et al.* (2003) a 40% change in MHC (from α-MHC to β-MHC) only resulted in a 20% reduction in V_{MAX}. Moreover, previous work has demonstrated that the V_{MAX} in unregulated *in vitro* motility assays is not affected by small changes in MHC isoform composition (Cuda *et al.* 1997). Therefore, even if there was a small amount of undetected α-MHC present, which varied between the gestational ages, it is unlikely to be responsible for the ~50% reduction in V_{MAX} that was observed between the 101 and 134 day samples. Another possible explanation for the changes in cross-bridge kinetics is either an altered isoform or phosphorylation state of the myosin light chains (Karabina *et al.* 2015). The mechanism responsible for the observed change in cross-bridge kinetics throughout human fetal heart development deserves future investigation.

Changes to the calcium sensitivity of the myofilament affect the activation kinetics and the duration of the initial, slow phase of relaxation (Poggesi *et al.* 2005; Kreutziger *et al.* 2011). A decrease in calcium sensitivity caused by a change in the properties of TnC could cause a decrease in the rate of activation (Kreutziger *et al.* 2011). However, the resulting decrease in calcium sensitivity we see in the human fetal heart is instead accompanied by a slight increase in the rate of activation. The duration of the slow phase is an indication of the thin filament 'on' period and this shortens between 59 and ~100 days of gestation. A shorter thin filament 'on' period may be consistent with lower calcium sensitivity (Kreutziger *et al.* 2011). We hypothesize that this shorter filament 'on' period is the result of either (1) decreased thin filament compliance, caused by more tightly bound thick and thin filaments, resulting in better translation of one troponin subunit turning 'off' affecting its neighbour; (2) a change in TnI isoform, switching to the adult cTnI isoform from the fetal cardiac/ssTnI isoform; or (3) better thin filament regulation of acto-myosin binding, caused by a higher density of TnC, resulting in less cross-bridge binding in the absence of calcium. We see evidence for the second hypothesis – that these changes to kinetics and Ca^{2+} sensitivity correlate with the proportion of ssTnI to cTnI – in both our data and in previous work on animal models of development. Fetal sheep hearts (Posterino *et al.* 2011) and fetal mouse hearts (Siedner *et al.* 2003) demonstrate continuous increases in the proportion of cTnI to total TnI, which has been correlated with decreased Ca^{2+} sensitivity of contraction (McAuliffe & Robbins, 1991; Siedner *et al.* 2003; Krüger *et al.* 2006; Posterino *et al.* 2011). Here, we also report an elevated (compared with previously reported adult) but decreasing calcium sensitivity as gestational age increases in the human fetal heart myofibrils. Additionally, similar to studies in other mammalian models of development, we also observed a steady increase in the amount of cTnI throughout gestation. The high proportion of ssTnI in the fetal heart is probably responsible for the increased Ca^{2+} sensitivity of fetal cardiac myofibrils compared with adults, and the shift from ssTnI to cTnI as the fetal human heart develops correlates with the loss of Ca^{2+} sensitivity that was observed. However, we cannot rule out the contribution of structural changes, or a change in TnC density may affect the contractile kinetics throughout development.

Future directions

This study provides an initial report on the contractile and structural properties of human fetal heart myofibrils. Future studies should include increasing the number of fetal heart samples at earlier (<100 days) and later (>116 days) gestation stages to increase the robustness of the data set shown here. Additionally, while these studies were limited to the left ventricle, the atria are known to carry far more α-MHC, which is implicated in several forms of genetically based congenital heart defects, and would be an important part of the fetal heart to study in the future. Currently there is considerable focus on the use of *in vitro* cultured cardiomyocytes (Burridge *et al.* 2015) to test potential therapeutics (Korte *et al.* 2011) and model inherited cardiomyopathies (Eschenhagen *et al.* 2015). However, the state of contractile maturity of these *in vitro* cultured cardiomyocytes is unknown. Therefore, future work could compare human-induced pluripotent stem cell-derived cardiomyocytes (hiPSC-CMs) with human fetal cardiac samples from both atria and ventricle tissues to assist in understanding the developmental age range these cells can attain in culture.

Limitations

This study was limited by the samples obtained; tissues samples were small in size, with limited maternal data. In-depth analysis on structure, proteomics and kinetics could not be studied with the limited number, quality and size of the samples obtained for these studies. As outlined in Table 1, samples were of both sexes, multiple ethnicities and, moreover, subjected to different conditions during gestation, which could have had unknown effects on the kinetics and force production. It is apparent in some samples, such as the single sample from 134 days *vs.* the two at 130 days, that variability between samples was large. This limited our ability to make definitive conclusions and rigorously test specific hypotheses regarding changes with increasing gestational age. While we were limited in our ability to obtain a similar number of samples at individual gestational ages, the data are consistent to the point that we can make some preliminary conclusions, and comparison over a broad range of ages can be used as a framework for more in-depth studies in the future.

References

Anderson PA, Malouf NN, Oakeley AE, Pagani ED & Allen PD (1991). Troponin T isoform expression in humans. A comparison among normal and failing adult heart, fetal heart, and adult and fetal skeletal muscle. *Circ Res* **69**, 1226–1233.

Belus A, Piroddi N, Scellini B, Tesi C, Amati GD, Girolami F, Yacoub M, Cecchi F, Olivotto I & Poggesi C (2008). The familial hypertrophic cardiomyopathy-associated myosin mutation R403Q accelerates tension generation and relaxation of human cardiac myofibrils. *J Physiol* **586**, 3639–3644.

Brenner B & Eisenberg E (1986). Rate of force generation in muscle: correlation with actomyosin ATPase activity in solution. *Proc Natl Acad Sci USA* **83**, 3542–3546.

Brooks PA, Khoo NS & Hornberger LK (2014). Systolic and diastolic function of the fetal single left ventricle. *J Am Soc Echocardiogr* **27**, 972–977.

Burridge PW, Diecke S, Matsa E, Sharma A, Wu H & Wu JC (2015). Modeling cardiovascular diseases with patient-specific human pluripotent stem cell-derived cardiomyocytes. In *Methods in Molecular Biology*. Humana Press. DOI: 10.1007/7651_2015_196.

Clemmens EW, Entezari M, Martyn DA & Regnier M (2005). Different effects of cardiac versus skeletal muscle regulatory proteins on in vitro measures of actin filament speed and force. *J Physiol* **566**, 737–746.

Clemmens EW & Regnier M (2004). Skeletal regulatory proteins enhance thin filament sliding speed and force by skeletal HMM. *J Musc Res Cell Motil* **25**, 515–525.

Colomo F, Piroddi N, Poggesi C, te Kronnie G & Tesi C (1997). Active and passive forces of isolated myofibrils from cardiac and fast skeletal muscle of the frog. *J Physiol* **500**, 535–548.

Cuda G, Pate E, Cooke R & Sellers JR (1997). In vitro actin filament sliding velocities produced by mixtures of different types of myosin. *Biophys J* **72**, 1767–1779.

Elmstedt N, Ferm-Widlund K, Lind B, Brodin L-Å & Westgren M (2012). Fetal cardiac muscle contractility decreases with gestational age: a color-coded tissue velocity imaging study. *Cardiovasc Ultrasound* **10**, 19.

Elmstedt N, Johnson J, Lind B, Ferm-Widlund K, Herling L, Westgren M & Brodin L-A (2013). Reference values for fetal tissue velocity imaging and a new approach to evaluate fetal myocardial function. *Cardiovasc Ultrasound* **11**, 29.

Eschenhagen T, Mummery C & Knollmann BC (2015). Modelling sarcomeric cardiomyopathies in the dish: from human heart samples to iPSC cardiomyocytes. *Cardiovasc Res* **105**, 424–438.

Fabiato A (1988). Computer programs for calculating total from specified free or free from specified total ionic concentrations in aqueous solutions containing multiple metals and ligands. *Meth Enzymol* **157**, 378–417.

Gordon AM, LaMadrid MA, Chen Y, Luo Z & Chase PB (1997). Calcium regulation of skeletal muscle thin filament motility in vitro. *Biophys J* **72**, 1295–1307.

Van Hees HWH, van der Heijden HFM, Ottenheijm CAC, Heunks LMA, Pigmans CJC, Verheugt FWA, Brouwer RMHJ & Dekhuijzen PNR (2007). Diaphragm single-fiber weakness and loss of myosin in congestive heart failure rats. *Am J Physiol Heart Circ Physiol* **293**, H819–H828.

Homsher E, Wang F & Sellers JR (1992). Factors affecting movement of F-actin filaments propelled by skeletal muscle heavy meromyosin. *Am J Physiol* **262**, C714–C723.

Karabina A, Kazmierczak K, Szczesna-Cordary D & Moore JR (2015). Myosin regulatory light chain phosphorylation enhances cardiac β-myosin in vitro motility under load. *Arch Biochem Biophys* **580**, 14–21.

Kim HD, Kim DJ, Lee IJ, Rah BJ, Sawa Y & Schaper J (1992). Human fetal heart development after mid-term: morphometry and ultrastructural study. *J Mol Cell Cardiol* **24**, 949–965.

Korte FS, Dai J, Buckley K, Feest ER, Adamek N, Geeves MA, Murry CE & Regnier M (2011). Upregulation of cardiomyocyte ribonucleotide reductase increases intracellular 2 deoxy-ATP, contractility, and relaxation. *J Mol Cell Cardiol* **51**, 894–901.

Korte FS, Feest ER, Razumova MV, Tu A-Y & Regnier M (2012). Enhanced Ca^{2+} binding of cardiac troponin reduces sarcomere length dependence of contractile activation independently of strong cross-bridges. *Am J Physiol Heart Circ Physiol* **303**, H863–H870.

Krenz M, Sanbe A, Bouyer-Dalloz F, Gulick J, Klevitsky R, Hewett TE, Osinska HE, Lorenz JN, Brosseau C, Federico A, Alpert NR, Warshaw DM, Perryman MB, Helmke SM & Robbins J (2003). Analysis of myosin heavy chain functionality in the heart. *J Biol Chem* **278**, 17466–17474.

Kreutziger KL, Piroddi N, McMichael JT, Tesi C, Poggesi C & Regnier M (2011). Calcium binding kinetics of troponin C strongly modulate cooperative activation and tension kinetics in cardiac muscle. *J Mol Cell Cardiol* **50**, 165–174.

Kreutziger KL, Piroddi N, Scellini B, Tesi C, Poggesi C & Regnier M (2008). Thin filament Ca^{2+} binding properties and regulatory unit interactions alter kinetics of tension development and relaxation in rabbit skeletal muscle. *J Physiol* **586**, 3683–3700.

Kron SJ, Toyoshima YY, Uyeda TQ & Spudich JA (1991*a*). Assays for actin sliding movement over myosin-coated surfaces. *Methods Enzymol* **196**, 399–416.

Kron SJ, Uyeda TQ, Warrick HM & Spudich JA (1991*b*). An approach to reconstituting motility of single myosin molecules. *J Cell Sci Suppl* **14**, 129–133.

Krüger M, Kohl T & Linke WA (2006). Developmental changes in passive stiffness and myofilament Ca^{2+} sensitivity due to titin and troponin-I isoform switching are not critically triggered by birth. *Am J Physiol Heart Circ Physiol* **291**, H496–H506.

Lamers WH, Virágh S, Wessels A, Moorman AF & Anderson RH (1995). Formation of the tricuspid valve in the human heart. *Circulation* **91**, 111–121.

Luewan S, Tongprasert F, Srisupundit K, Traisrisilp K & Tongsong T (2014). Reference ranges of myocardial performance index from 12 to 40 weeks of gestation. *Arch Gynecol Obstet* **290**, 859–865.

Margossian SS & Lowey S (1982). Preparation of myosin and its subfragments from rabbit skeletal muscle. *Methods Enzymol* **85**, 55–71.

Martyn DA, Chase PB, Regnier M & Gordon AM (2002). A simple model with myofilament compliance predicts activation-dependent cross-bridge kinetics in skinned skeletal fibers. *Biophys J* **83**, 3425–3434.

McAuliffe JJ & Robbins J (1991). Troponin T expression in normal and pressure-loaded fetal sheep heart. *Pediatr Res* **29**, 580–585.

Moussavi-Harami F, Razumova MV, Racca AW, Cheng Y, Stempien-Otero A & Regnier M (2015). 2-Deoxy adenosine triphosphate improves contraction in human end-stage heart failure. *J Mol Cell Cardiol* **79**, 256–263.

Pardee JD & Spudich JA (1982). Purification of muscle actin. *Methods Enzymol* **85**, 164–181.

Piroddi N, Belus A, Scellini B, Tesi C, Giunti G, Cerbai E, Mugelli A & Poggesi C (2007). Tension generation and relaxation in single myofibrils from human atrial and ventricular myocardium. *Pflugers Arch* **454**, 63–73.

Poggesi C, Tesi C & Stehle R (2005). Sarcomeric determinants of striated muscle relaxation kinetics. *Pflugers Arch* **449**, 505–517.

Posterino GS, Dunn SL, Botting KJ, Wang W, Gentili S & Morrison JL (2011). Changes in cardiac troponins with gestational age explain changes in cardiac muscle contractility in the sheep fetus. *J Appl Physiol* **111**, 236–243.

Purcell IF, Bing W & Marston SB (1999). Functional analysis of human cardiac troponin by the in vitro motility assay: comparison of adult, foetal and failing hearts. *Cardiovasc Res* **43**, 884–891.

Racca AW, Beck AE, Bamshad MJ & Regnier M (2014). Differences in activation and relaxation kinetics of human fetal skeletal and cardiac myofibrils. *Biophys J* **106**, 562a.

Racca AW, Beck AE, McMillin MJ, Korte FS, Bamshad MJ & Regnier M (2015). The embryonic myosin R672C mutation that underlies Freeman-Sheldon syndrome impairs cross-bridge detachment and cycling in adult muscle. *Hum Mol Genet* **24**, 3348–3358.

Racca AW, Beck AE, Rao VS, Flint GV, Lundy SD, Born DE, Bamshad MJ & Regnier M (2013). Contractility and kinetics of human fetal and human adult skeletal muscle. *J Physiol* **591**, 3049–3061.

Rao V, Cheng Y, Lindert S, Wang D, Oxenford L, McCulloch AD, McCammon JA & Regnier M (2014). PKA phosphorylation of cardiac troponin I modulates activation and relaxation kinetics of ventricular myofibrils. *Biophys J* **107**, 1196–1204.

Razumova MV, Shaffer JF, Tu A-Y, Flint GV, Regnier M & Harris SP (2006). Effects of the N-terminal domains of myosin binding protein-C in an in vitro motility assay: evidence for long-lived cross-bridges. *J Biol Chem* **281**, 35846–35854.

Regnier M, Rivera AJ, Chen Y & Chase PB (2000). 2-deoxy-ATP enhances contractility of rat cardiac muscle. *Circ Res* **86**, 1211–1217.

Reiser PJ, Portman MA, Ning XH & Schomisch Moravec C (2001). Human cardiac myosin heavy chain isoforms in fetal and failing adult atria and ventricles. *Am J Physiol Heart Circ Physiol* **280**, H1814–H1820.

Rolph TP, Jones CT & Parry D (1982). Ultrastructural and enzymatic development of fetal guinea pig heart. *Am J Physiol* **243**, H87–H93.

Sasse S, Brand NJ, Kyprianou P, Dhoot GK, Wade R, Arai M, Periasamy M, Yacoub MH & Barton PJ (1993). Troponin I gene expression during human cardiac development and in end-stage heart failure. *Circ Res* **72**, 932–938.

Sheldon CA, Friedman WF & Sybers HD (1976). Scanning electron microscopy of fetal and neonatal lamb cardiac cells. *J Mol Cell Cardiol* **8**, 853–862.

Siedner S, Krüger M, Schroeter M, Metzler D, Roell W, Fleischmann BK, Hescheler J, Pfitzer G & Stehle R (2003). Developmental changes in contractility and sarcomeric proteins from the early embryonic to the adult stage in the mouse heart. *J Physiol* **548**, 493–505.

Spudich JA, Pardee JD, Simpson PA, Yamamoto K, Kuczmarski ER & Stryer L (1982). Actin and myosin: control of filament assembly. *Phil Trans R Soc B* **299**, 247–261.

Tesi C, Piroddi N, Colomo F & Poggesi C (2002). Relaxation kinetics following sudden Ca^{2+} reduction in single myofibrils from skeletal muscle. *Biophys J* **83**, 2142–2151.

De Tombe PP, Belus A, Piroddi N, Scellini B, Walker JS, Martin AF, Tesi C & Poggesi C (2007). Myofilament calcium sensitivity does not affect cross-bridge activation-relaxation kinetics. *Am J Physiol Regul Integr Comp Physiol* **292**, R1129–R1136.

Williams CD, Regnier M & Daniel TL (2010). Axial and radial forces of cross-bridges depend on lattice spacing. *PLoS Comput Biol* **6**, e1001018.

Williams CD, Salcedo MK, Irving TC, Regnier M & Daniel TL (2013). The length–tension curve in muscle depends on lattice spacing. *Proc Biol Sci* **280**, 20130697.

Additional information

Competing interests

None declared.

Author contributions

All experiments were performed at the University of Washington in Seattle. A.W.R. designed and performed experiments, analysed and interpreted data, and wrote the manuscript. J.M.K. contributed to and helped design the proteomics assays, and the writing and editing of the manuscript. J.M.P contributed to myofibril experiments and edited the manuscript. Y.H.C. contributed to myofibril experiments. A.E.B. contributed to the acquisition of the human fetal tissues. F.M.H contributed to obtaining human adult samples, analysing the myofibril data and editing the manuscript. M.J.B. contributed to overall study design and critically reviewed the manuscript. M.R. contributed to overall study design, interpretation of results and writing of the manuscript. All authors approved the final version of the manuscript for publication.

Acknowledgements

The content does not necessarily represent the official views of the National Institutes of Health. Fetal samples for this project were provided by the project entitled 'Laboratory of Developmental Biology,' supported by NIH Award Number 5R24HD0008836 from the Eunice Kennedy Shriver National Institute of Child Health & Human Development. Electron microscopy imaging was done through the Vision Research Center Core at the University of Washington, funded by NIH award number P30 EY01730, with the assistance of Edward Parker. We would also like to thank Dr Stempien-Otero for allowing us access to the human adult tissue. This work was supported by NIH awards HL65497, HL11197 (M.R.), HD048895 (M.J.B. & M.R.), HD057331 (A.E.B.) and F31AR063000 (A.W.R.). J.M.K. is supported by a Heart and Stroke Foundation of Canada Postdoctoral Fellowship.